

Charge asymmetries in $\gamma\gamma \rightarrow \mu^+\mu^- + \nu_\mu\bar{\nu}_\mu$ / $\gamma\gamma \rightarrow W^\pm\mu^\mp + \nu_\mu$ with polarized photons

D. A. Anipko,¹ M. Cannoni,^{2,3} I. F. Ginzburg,¹ O. Panella³ and A. V. Pak¹

¹ *Sobolev Institute of Mathematics and Novosibirsk
State University, Novosibirsk, 630090, Russia*

² *Dipartimento di Fisica, Università degli Studi di Perugia,
Via A. Pascoli, I-06123, Perugia, Italy and*

³ *Istituto Nazionale di Fisica Nucleare, Sezione di Perugia,
Via A. Pascoli, I-06123, Perugia, Italy*

(Dated: June 16, 2003)

Abstract

It is shown that the difference in the distributions of positive (μ^+) and negative charged leptons (μ^-) in reactions $\gamma\gamma \rightarrow \mu^+\mu^- + \nu\bar{\nu}$ and $\gamma\gamma \rightarrow W^\pm\mu^\mp + \nu(\bar{\nu})$ at $\sqrt{s} > 200$ GeV leads to observable *charge asymmetry* of muons which is sensitive to New Physics effects.

Talk presented by I. F. Ginzburg at Photon 2003: International Conference on the Structure and Interactions of the Photon and 15th International Workshop on Photon-Photon Collisions, Frascati, Italy, 7-11 Apr 2003.

I. INTRODUCTION

The Photon Collider [1] option of the next generation linear colliders (LC) [2] offers the opportunity to study with high precision the physics of gauge bosons of the Standard Model with sensitivity to effects coming from New Physics. High energy photons are produced by Compton back-scattering of laser photons from high energy electron (or positron) beams: they will not be monochromatic but will have an energy spectrum. The high energy part of this spectrum will mainly include photons with definite helicity $\lambda_i \approx \pm 1$.

The SM cross section of $\gamma\gamma \rightarrow W^+W^-$ at energies greater than 200 GeV is about 80 pb and remains constant up to higher energies of interest [3]. This large cross section will ensure very high event rates. When initial photons are circularly polarized one expects different momentum distributions between the positively and negatively charged leptons from the decay of the W gauge bosons which is referred to as a *charge asymmetry*. A qualitative discussion of the mechanism originating charge asymmetries is given in Sec. II.

One expects that a study of charge asymmetries will be a sensitive tool to study New Physics effects. Therefore, all mechanisms leading to this asymmetry should be investigated in detail. In the following we study the charge asymmetry in the Standard Model (SM) and make preliminary considerations on how these asymmetries change due to some possible effects of New Physics.

Numerical results (including all plots) have been obtained with the CompHEP package [4] in a version which allows to set the initial photons in a definite helicity state and to implement realistic photon energy spectra. The following cuts are applied below: (1) an angular cut on the muons scattering angles given by $\pi - \theta_0 > \theta > \theta_0$, with $\theta_0 = 10$ mrad (corresponding to the TESLA detector angular limitations); (2) a cut on muons transverse momentum $p_\perp > 10$ GeV, both on each muon and on the couple of muons. These two cuts help to suppress the background.

We discuss two effects of charge asymmetry:

- Asymmetry of μ^+ and μ^- momenta in each event, averaged over events in the process $\gamma\gamma \rightarrow \mu^+\mu^-\nu\bar{\nu}$ where both muons are recorded.
- Difference in distributions of μ^+ and μ^- in the processes $\gamma\gamma \rightarrow W^+\mu^-\bar{\nu}$, $\gamma\gamma \rightarrow W^-\mu^+\nu$, where we assume W reconstruction via effective mass of two jets ($W \rightarrow q\bar{q}$ mode) or its lepton decay. Most of the numerical results presented concern this last approach.

◇ In the following we mark polarization of an initial state, e.g. $(+-)$, that means $\lambda_1 = +1$, $\lambda_2 = -1$, where λ_1 and λ_2 are helicities of photons moving in the positive and negative direction of the collision axis (z axis) respectively.

II. DIAGRAMS AND QUALITATIVE DESCRIPTION

• In SM, at the tree level, the process $\gamma\gamma \rightarrow \mu^+\mu^-\nu\bar{\nu}$ is described by 19 diagrams. We subdivide them in 5 types, shown in Fig. 1 (a similar classification was given also in Ref. [5]). The collection of diagrams within each type is obtained from those shown in the figure with the exchange $+ \leftrightarrow -$, $\nu \leftrightarrow \bar{\nu}$ and permutations of photons. In the estimates of cross sections we denote $B = Br(W \rightarrow \mu\nu)$ and $B_Z = Br(Z \rightarrow \nu\bar{\nu})$.

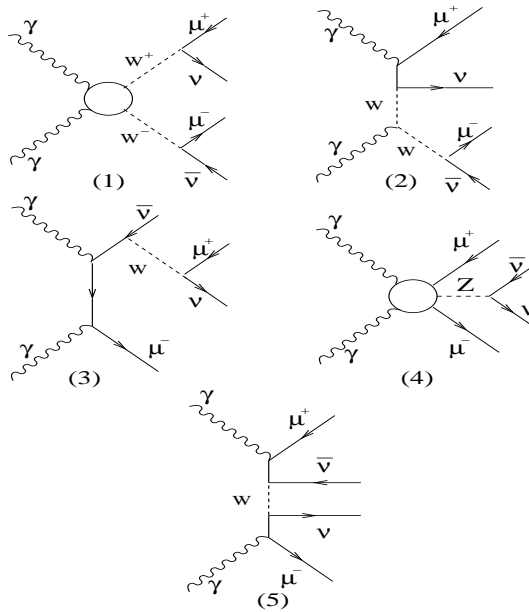


FIG. 1: Different classes of tree level Feynman diagrams contributing to $\gamma\gamma \rightarrow \mu^+\mu^-\nu\bar{\nu}$.

- (1) 3 double-resonant diagrams (DRD) of Fig. 1(1) describe WW production and decay. Their contribution to the total cross section can be evaluated as $\sigma_d \sim (\alpha^2/M_W^2)B^2$, numerically it accounts for $\approx 70\%$ of the cross section.
- (2) 4 single-resonant diagrams of Fig. 1(2) with W exchange in t -channel. The corresponding contribution is estimated as $\sigma_{sW} \sim (\alpha^3/M_W^2)B \sim \alpha\sigma_d/B$.

- (3) 4 single resonant diagrams with μ exchange in t -channel (gauge boson bremsstrahlung), Fig. 1(3). Their contribution to the total cross section is estimated as: $\sigma_{s\mu} \sim (\alpha^3/s)B \sim \alpha\sigma_d M_W^2/(Bs)$; numerically they provide less than 1%.
- (4) 6 diagrams with radiation of Z boson in the process $\gamma\gamma \rightarrow \mu^+\mu^-$, Fig. 1(4) give asymptotic contribution $\sigma_Z \sim (\alpha^3/s)B_Z \sim \alpha\sigma_d M_W^2 B_Z/(B^2s)$; numerically they amount less than 1%.
- (5) 2 non-resonant diagrams Fig. 1(5) with $\sigma_n \sim \alpha^4/M_W^2 \sim \alpha^2\sigma_d M_W^2/(B^2s)$; numerically they amount less than 1%.

Our analytical estimates are based on the equations for $2 \rightarrow 2$ processes at $s \gg M_W^2$, assuming for the SM gauge couplings $g^2 \sim g'^2 \sim \alpha$. Numerical estimates are obtained at $\sqrt{s} = 500$ GeV with CompHEP in the Feynman gauge for the squared contributions of each group. The value of the interference with the dominant DRD is roughly the same, since DRD are large only in two regions of the final phase space corresponding to W resonances. The other contributions do not have these two peaks.

The asymmetry is present in the double-resonant contribution. There are no reasons to expect the other diagrams to contribute to the asymmetry more than their relative contributions to the cross section. Note that the contribution of diagrams of group 5 is at the level of radiative corrections to the dominant contribution. The precision provided by including this contribution is beyond the accuracy of the tree approximation.

- The process $\gamma\gamma \rightarrow W^+\mu^-\bar{\nu}$ is described by only the first 3 groups of diagrams.

Therefore, in the following qualitative discussion we refer to the double resonant contribution while all numerical results and plots are obtained for the complete set of 19 diagrams.

Let us describe the expected picture for double resonant contribution. (i) At $\sqrt{s} > 200$ GeV the $\gamma\gamma \rightarrow W^+W^-$ cross section practically does not depend on photon polarizations. (ii) In the $\gamma\gamma \rightarrow W^+W^-$ process, the W gauge bosons are distributed mainly around the forward and backward directions with mean transverse momentum $\sim M_W$ ($d\sigma \propto 1/(p_\perp^2 + M_W^2)^2$ [3]). (iii) In this process helicity conservation holds approximately (see helicity amplitudes in [6]). The helicity of W^\pm moving in the positive direction of z axis $\lambda_{W_1} \approx \lambda_1$, while $\lambda_{W_2} \approx \lambda_2$, is independent on the charge sign of W . (iv) Let the z' -axis be directed along the W momentum (\mathbf{p}_W) and $\varepsilon \approx M_W/2$ and $p_{z'}$ are the energy and the longitudinal momentum of μ in the W rest frame. It is straightforward to show that the

distribution of muons from the decay of the W gauge boson with charge $e = \pm 1$ and helicity $\lambda = \pm 1$ in its rest frame is ¹: $\propto (\varepsilon - e\lambda p_{z'})^2$. In other words, the distribution of muons from the decay of W^\pm has a peak along \mathbf{p}_W if $e\lambda_W = -1$ and opposite to \mathbf{p}_W when $e\lambda_W = +1$. These distributions are boosted easily to the $\gamma\gamma$ collision frame. For example when photons have a $(--)$ helicity state, produced μ^+ are distributed around the upper value of their longitudinal momentum (both in the forward and backward direction), while produced μ^- are concentrated near the zero value of their longitudinal momentum. This boost makes the distribution in p_\perp wider in the first case and narrower in the second case.

III. NUMERICAL RESULTS

We present here the first results, reporting the distributions of muons $\partial^2\sigma/(\partial p_\parallel\partial p_\perp)$ (with p_\parallel the component of \vec{p}_{μ^\pm} parallel to the collision axis (taken to be the z axis) and $p_\perp = \sqrt{p_x^2 + p_y^2}$ the transverse momentum). Fig. 2 shows such muon distributions in the (p_\parallel, p_\perp) plane for a $(--)$ initial photon polarization state with monochromatic photons at different values of the energy. Fig. 2 clearly shows the charge asymmetry: *a strong difference in the distributions of μ^- and μ^+* in accordance with qualitative description given above. The absolute value of charge asymmetry effect decreases with energy due to the increasing importance of the applied cuts.

In all figures and tables below we consider $\sqrt{s_{\gamma\gamma}} = 500$ GeV for the monochromatic case and $\sqrt{s_{ee}} = 500$ GeV, $x = 4.8$ for "realistic" spectra.

In Fig. 3 we show two-dimensional level lines, for different initial helicity states and monochromatic photons. Note that the scales of effect in the graphs with μ^- for $(--)$ case differ from other cases by a factor of seven. Due to CP conservation, the μ^\pm distributions for $(--)$ case coincide with μ^\mp distribution for $(++)$ case. The obtained distributions in the (p_\parallel, p_\perp) plane have the form which corresponds to the qualitative picture outlined in Sec. II.

To make a more transparent analysis, we consider the normalized mean values of longitudinal and transverse momenta of μ^- and μ^+ , determined considering the longitudinal momentum of μ in the forward hemisphere ($p_\parallel > 0$), and take their relative difference as a

¹ The transverse momenta of muons are distributed roughly isotropically relative to W momentum within the interval $p_\perp < m_W/2$.

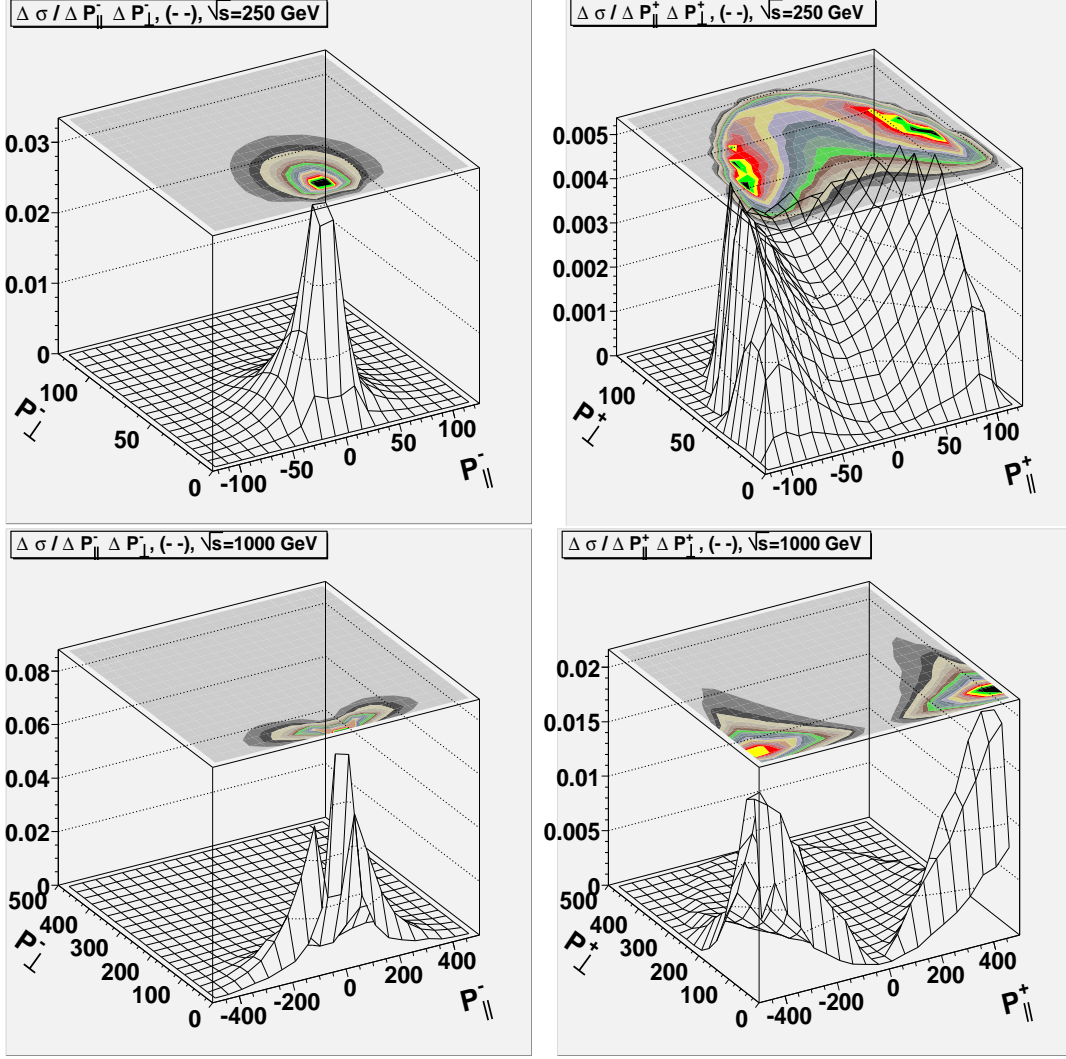


FIG. 2: The distributions in the $(p_{||}, p_{\perp})$ plane for $(--)$ helicity of colliding photons: μ^- on the left, μ^+ on the right: $\sqrt{s} = 250$ GeV (top) and $\sqrt{s} = 1000$ GeV (bottom). Monochromatic beams.

measure of the charge asymmetry:

$$\begin{aligned}
 P_{L+}^{\pm} &= \frac{\int p_{||}^{\pm} d\sigma}{E_{\gamma max} \int d\sigma}, & P_{T+}^{\pm} &= \frac{\int p_{\perp}^{\pm} d\sigma}{E_{\gamma max} \int d\sigma}, \\
 \Delta_L &= \frac{P_{L+}^- - P_{L+}^+}{P_{L+}^- + P_{L+}^+}, & \Delta_T &= \frac{P_{T+}^- - P_{T+}^+}{P_{T+}^- + P_{T+}^+}.
 \end{aligned} \tag{1}$$

We have calculated these quantities for the process $\gamma\gamma \rightarrow W\mu\nu$ at $\sqrt{s} = 500$ GeV $\Rightarrow E_{\gamma max} = 250$ GeV for monochromatic case and for $\sqrt{s_{ee}} = 500$ GeV $\Rightarrow E_{\gamma max} = 207$ GeV for the "realistic" photon spectra. In tables below the parameter N takes two values N=L

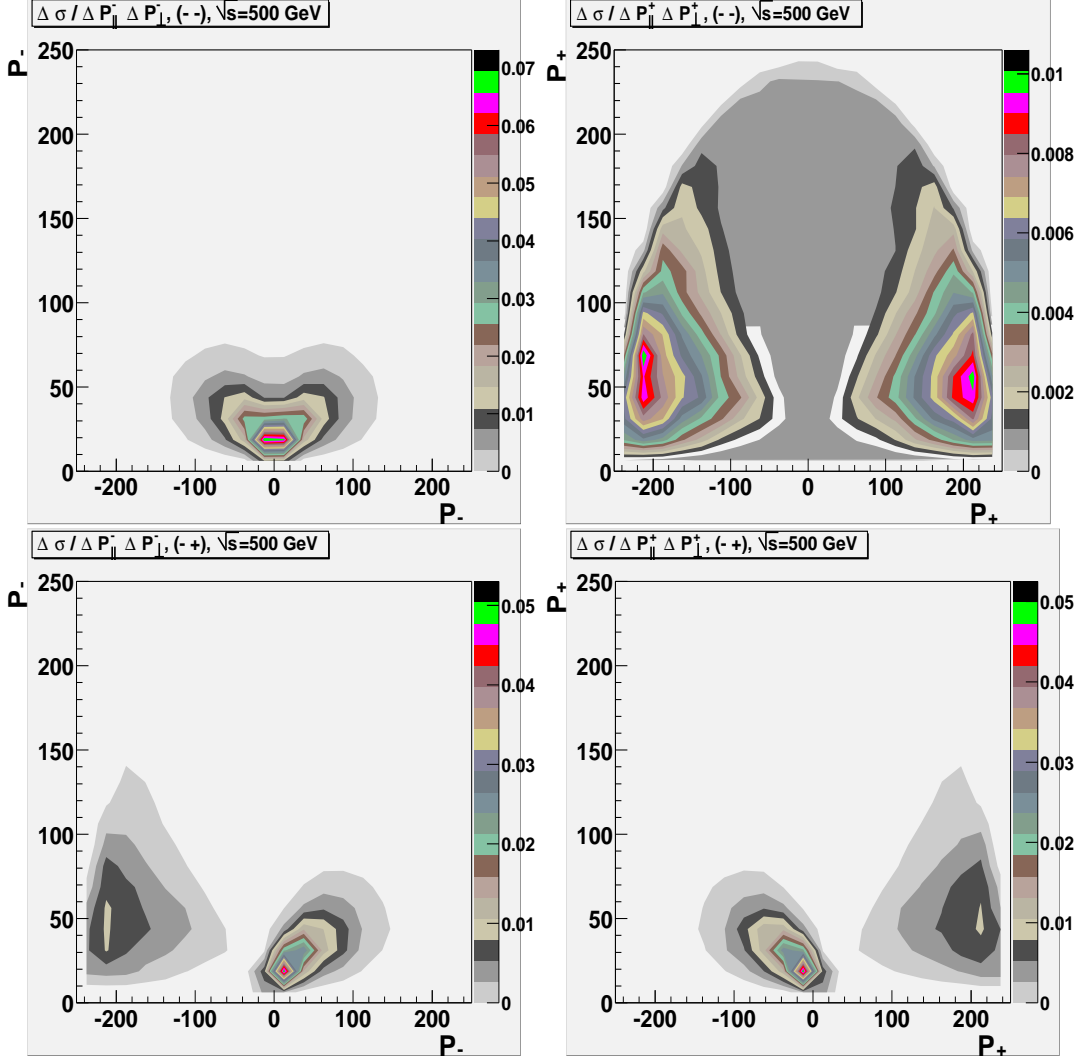


FIG. 3: Distributions in the $(p_{\parallel}, p_{\perp})$ plane (pb/bin). Left – μ^{-} , right – μ^{+} ; from the top: $(--)$, $(-+)$ – helicities of colliding photons. Monochromatic beams.

(longitudinal) and N=T (transverse). Table 1 presents the values of the asymmetries for different photon polarizations in the monochromatic case. The $(++)$ case coincides with the $(--)$ one with the exchange $\mu^{+} \rightarrow \mu^{-}$. For $(+-)$ initial state the pictures in forward and backward hemispheres are different. The latter coincide with that for the forward hemisphere for $(-+)$ initial state with the exchange $\mu^{+} \leftrightarrow \mu^{-}$.

One can see that the values of the asymmetry is typically 20-50%. That is *a huge and easily observable effect*.

Note that the scale of longitudinal distributions is given by the initial photon energy

TABLE I: SM. Monochromatic case.

$(\lambda_1 \lambda_2) N$	P_{N+}^-	P_{N+}^+	Δ_N
$(- -) N=L$	0.605	0.191	0.520
$N=T$	0.353	0.160	0.374
$(+ -) N=L$	0.229	0.571	-0.427
$N=T$	0.167	0.262	-0.221
$(- +) N=L$	0.233	0.631	-0.461
$N=T$	0.179	0.283	-0.223

while the scale for transverse distributions is given by the W mass. Thus, the transverse asymmetries are smaller than the longitudinal ones.

- **Effect of photon non-monochromaticity.** Photon beams at the Photon collider will be non-monochromatic. The energy spectra are well known for high energies where the approximation of Ref. [7] works well but the low-energy part will differ depending on technological details. Fortunately, these photons are unpolarized and do not contribute to the asymmetry. So that, in all Tables 2–4 we used "realistic" photon spectra with $\rho = 1$ from Ref. [7] for the high energy part, and from Ref. [1] with $\rho = 0$ for the low energy part (similar to that it was done in Ref. [8]). We assume here $x = 4.8$ for $e \rightarrow \gamma$ conversion which corresponds to the maximal value of photon energy $E_\gamma^m \approx 207$ GeV at $\sqrt{s_{ee}} = 500$ GeV. The resulting asymmetries are shown in the Table 2. The longitudinal asymmetry changes only weakly in comparison with the monochromatic case, while the transverse asymmetry

TABLE II: SM.

$(\lambda_1 \lambda_2) N$	P_{N+}^-	P_{N+}^+	Δ_N
$(- -) N=L$	0.499	0.150	0.536
$N=T$	0.382	0.178	0.364
$(+ -) N=L$	0.187	0.451	-0.415
$N=T$	0.198	0.272	-0.160
$(- +) N=L$	0.205	0.514	-0.436
$N=T$	0.219	0.300	-0.158

changes strongly. We verified that in the $(p_{\parallel}, p_{\perp})$ plane, relative to the monochromatic case, one can see a noticeable deviation in the phase space regions responsible for the asymmetry.

- Next, we consider the effect of **possible anomalous interactions of W -bosons**, parameterized by the usual anomalous magnetic moment $\Delta\kappa$ and the quadrupole moment λ in the trilinear and quartic vertices (with the same normalization as in Ref. [8]). We

TABLE III: SM with anomalous gauge boson interaction

$\Delta\kappa$	λ	$(\lambda_1 \lambda_2)$	N	P_{N+}^-	P_{N+}^+	Δ_N
0.1	0	$(--)$	L	0.498	0.150	0.537
			T	0.379	0.182	0.351
		$(+-)$	L	0.186	0.451	-0.416
			T	0.200	0.272	-0.152
		$(-+)$	L	0.204	0.510	-0.429
			T	0.221	0.300	-0.152
0	0.1	$(--)$	L	0.491	0.151	0.457
			T	0.388	0.177	0.378
		$(+-)$	L	0.190	0.457	-0.413
			T	0.192	0.270	-0.169
		$(-+)$	L	0.206	0.522	-0.438
			T	0.212	0.301	-0.173

calculated the asymmetries defined in Eq. (1) for large enough values of $\Delta\kappa$ and λ . The results are shown in the Table 3. Comparing with Table 2, one can see that the anomalous magnetic moment $\Delta\kappa$ changes the quantities $\Delta_{L,T}$ only weakly. One should study, whether any other variable is better to investigate the effects of this anomaly. On the other hand, the quadrupole moment λ changes Δ_L significantly at least in the $(--)$ case. Therefore, this asymmetry can be useful for the study of the λ anomaly.

- **Possible new particles.** To mimic the effect of new interactions and/or new particles, we consider a toy model with a "muon" having a mass of 40 GeV. The results are shown in Table 4. Comparing with Table 2, we conclude that the study of charge asymmetry can be a useful tool for the discovery of new particles.

TABLE IV: Toy model with $m_\mu = 40$ GeV

$(\lambda_1 \lambda_2) N$	P_{N+}^-	P_{N+}^+	Δ_N
(--) N=L	0.519	0.287	0.289
N=T	0.385	0.236	0.240
(+ -) N=L	0.325	0.569	-0.271
N=T	0.222	0.310	-0.201
(- +) N=L	0.295	0.545	-0.250
N=T	0.216	0.308	-0.175

IV. CHARGE ASYMMETRY OF MUONS IN EACH EVENT, $\gamma\gamma \rightarrow \mu^+\mu^-\nu\bar{\nu}$

The charge asymmetry in relative distributions of positive and negative muons can be a more useful instrument to hunt for New Physics. The first problem here is to find some representative variables in the 5-dimensional (\vec{p}_+, \vec{p}_-) phase space. For this purpose we consider the $\gamma\gamma \rightarrow \mu^+\mu^-\nu\bar{\nu}$ process with monochromatic photons. Fig. 4 presents the level

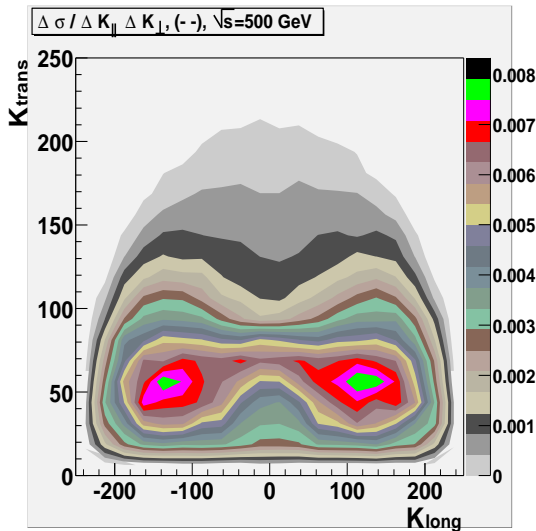


FIG. 4: Distribution in k_{\parallel}, k_{\perp} , monochromatic photons,

curves of the distribution in $\vec{k} = \vec{p}_+ + \vec{p}_-$, in its longitudinal and transverse component. In the *absence* of charge asymmetry this distribution would be centered around the point $(k_{\parallel}, k_{\perp}) = (0, 0)$. Clearly the charge asymmetry is quite large. Besides, we study various

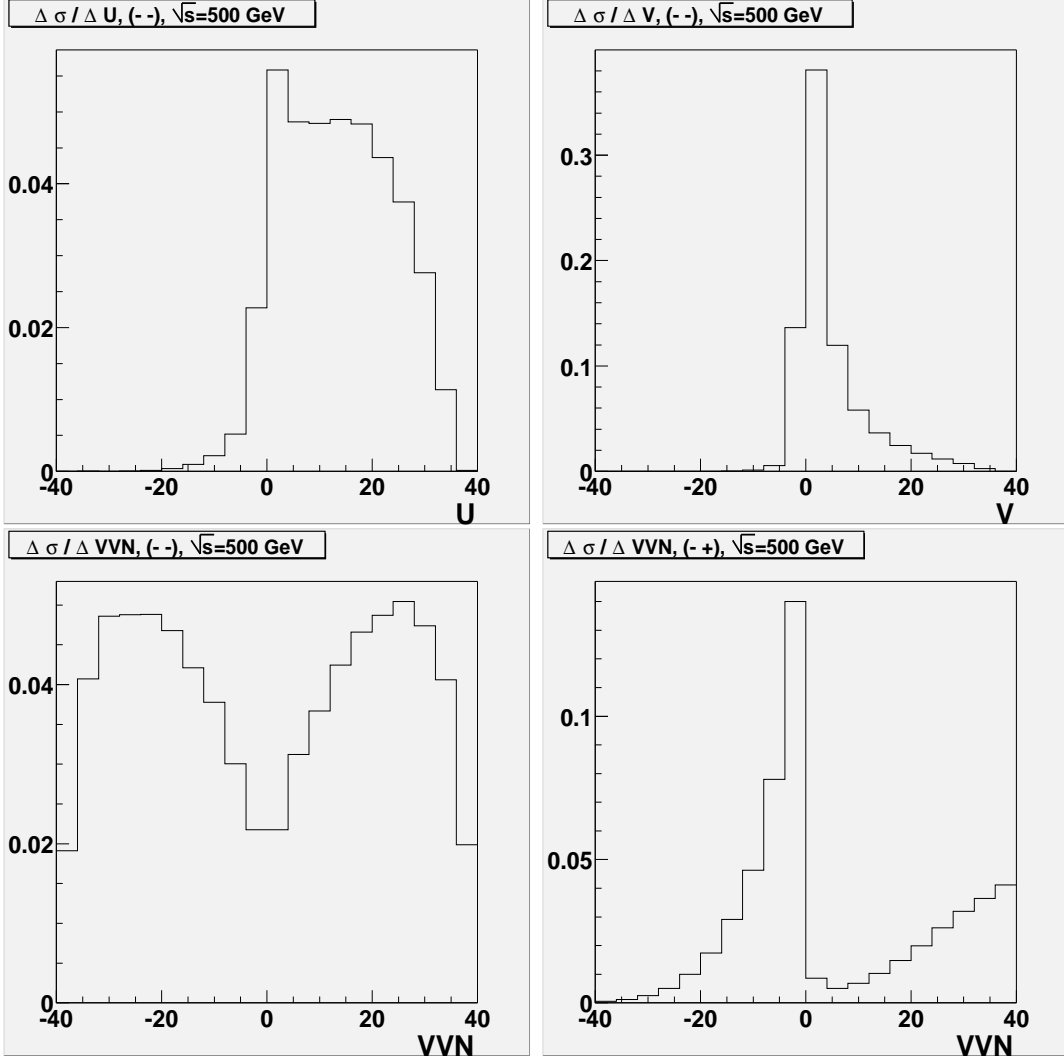


FIG. 5: Top panels: distribution in u and v for the $(- -)$ case. Bottom panels: distribution in vvn for $(- -)$ and $(- +)$ initial helicities.

“natural” dimensionless variables. In particular, we find useful to present distributions in following variables, Figure 5.

$$\begin{aligned}
 v &= \frac{4(p_{\perp+}^2 - p_{\perp-}^2)}{M_W^2}, & u &= \frac{4(p_{\parallel+}^2 - p_{\parallel-}^2)}{M_W^2}, \\
 vvn &= \frac{4(p_{\parallel+}\epsilon_+ - p_{\parallel-}\epsilon_-)}{M_W^2}.
 \end{aligned}
 \tag{2}$$

Fig. 3 shows that in the cases $(- -)$, $(+ +)$ distributions in the forward and backward hemispheres are identical. Therefore, in this case the variables u and v are useful while vvn can not be useful. Vice versa, for the $(+ -)$ case the variable vvn is useful while u and v

are not. The choice of some other variables and sensitivity to New Physics effects will be studied elsewhere.

V. DISCUSSION AND OUTLOOK

- The effects considered so far are identical for electrons and muons. So that, absolutely the same asymmetry will be observed in e^+e^- , $e^+\mu^-$, μ^+e^- distributions. Therefore, all these contributions should be gathered for a complete analysis. This will enhance the value of cross section for $\gamma\gamma \rightarrow \mu^+\mu^-\nu\bar{\nu}$ from 0.9 to 3.7 pb and for $\gamma\gamma \rightarrow W^+\mu^-\bar{\nu}$, etc. to 23.5 pb (millions of events per year).

- The contribution to the observable final state is given not only by the process $\gamma\gamma \rightarrow \mu^+\mu^-\nu\bar{\nu}$, but also by processes $\gamma\gamma \rightarrow \mu^+\mu^-\nu\bar{\nu} + \nu\bar{\nu}$ pairs. The most important of them will be, for example, $\gamma\gamma \rightarrow \tau^+\mu^-\nu\bar{\nu}$, etc. with subsequent decay $\tau \rightarrow \mu\nu\bar{\nu}$. The cross section of this process is 17% of those discussed above ($Br(\tau \rightarrow \mu\nu\bar{\nu})$ [9]) + 17% for the case with the change $\tau^+ \rightarrow \tau^-$, etc. +3% for $\gamma\gamma \rightarrow \tau^+\tau^-\nu\bar{\nu}$. Unfortunately, at the moment there are no regular methods for precise calculation of such processes like CompHEP or WHIZARD (6 or 8 particles in final state and very narrow intermediate state). We hope that the corresponding algorithm will be developed in a reasonable time using the fact that τ is a very narrow particle.

- We plan to calculate such a charge asymmetry in the case of existence of some new particles and interactions (e.g. MSSM).

Acknowledgments

This work is partially supported by grants RFBR 02-02-17884, NSh-2339.2003.2, INTAS 00-00679 and grant 015.02.01.16 Russian Universities and by the European Union under contract N. HPMF-CT-2000-00752. I. F. Ginzburg acknowledges support from the Landau Network – Centro Volta (Como) Italy, and from INFN Sezione di Perugia.

[1] I. F. Ginzburg, G. L. Kotkin, V. G. Serbo and V. I. Telnov, Nucl. Instrum. Meth. 205 (1983) 47;

- I. F. Ginzburg, G. L. Kotkin, S. L. Panfil, V. G. Serbo and V. I. Telnov, Nucl. Instrum. Meth. A 219 (1984) 5.
- [2] B. Badelek *et al.* [ECFA/DESY Photon Collider Working Group Collaboration], hep-ex/0108012.
- [3] I.F. Ginzburg, G.L. Kotkin, S.L. Panfil, V.G. Serbo, Nucl. Phys. B 228 (1983) 285.
- [4] A. Pukhov *et al.*, hep-ph/9908288.
- [5] E. Boos and T. Ohl, Phys. Lett. B 407 (1997) 161, hep-ph/9705374.
- [6] M.Baillargeon, G. Belanger, F. Boudjema. hep-ph/9405359
- [7] I.F. Ginzburg, G.L. Kotkin, Eur. Phys. J. C 13 (2000) 295.
- [8] D. A. Anipko, I. F. Ginzburg and A. V. Pak, hep-ph/0201072.
- [9] K. Hagiwara *et al.*, Phys. Rev. D 66, 010001 (2002)